

Production and Wear Optimization of an MSSA Reinforced Al-Si-Mg Composite: A Taguchi Approach

Ezekiel Otor OCHUOKPA

Danjuma Saleh YAWAS

Malachy Sumaila

Bassey Okon Samuel (✉ basseyokon59@gmail.com)

Ahmadu Bello University <https://orcid.org/0000-0001-9104-7063>

Research Article

Keywords: Composites, Aluminum Matrix Composites, Wear

Posted Date: February 10th, 2022

DOI: <https://doi.org/10.21203/rs.3.rs-1333622/v1>

License:  This work is licensed under a Creative Commons Attribution 4.0 International License. [Read Full License](#)

Abstract

In this study, Al-Si-Mg-MSSA composite is produced by reinforcing the aluminum alloy with mango seed shell ash (MSSA). For the development parameters of stirring time, processing temperature, MSSA content, and MSSA particle size, Taguchi design of experiment was employed for the optimization of the wear properties of the developed composites. The optimal wear rate of the MSSA reinforced Al-Si-Mg composite was obtained to be $0.001517\text{mm}^3/\text{N}/\text{m}$ at stirring time, processing temperature, MSSA content, and particle size of 60s, 720°C , 20%, and $25\mu\text{m}$. Analysis of variance also proved the significance of MSSA particles in the reduction of the wear rate of Al-Si-Mg alloys. The wear behavior of the developed composite was successfully modeled using regression analysis with a prediction accuracy of 90.32%.

1.0 Introduction

Aluminum metal matrix composites (AMCs) have found wide applications in our daily life because when in comparison with base aluminum alloy, they have exhibited good combinations of mechanical and tribological properties. With their unique properties, aluminum matrix composites have increasingly found application in industries like construction, automobile, aviation, etc. These unique properties such as low weight, high strength to weight ratio, low cost, low wear rate, etc. make it a better choice for materials such as polymer composites. In respect to other metal matrix composites, aluminum matrix composites (AMCs) have always been a better choice because of their corrosion resistance property, low density, good thermal conductivity, and low cost of production (Xie et al., 2021; Guo et al., 2021; Zhu et al., 2021; Wang et al., 2021).

Using the Acheson process, some of these synthetic materials like silicon carbide (SiC) are prepared where silica sand and carbon are charged in the electric furnace-based reactors as source materials (Raj, 2021). These processing techniques and the availability of these raw materials are a challenge in developing countries even though other authors have reported alternate processing methods like powder mixing, chemical vapor deposition, carbothermal reduction of silica, sol-gel processes, and also laser pyrolysis (Guo et al., 2021; Salur et al., 2021; Adediran et al., 2021). But all these methods also entail the use of advanced processing equipment which are not readily available in developing countries. The most cost-effective technique which poses no advanced equipment challenge is the carbothermal synthesis process which can be used in the production of silicon-based refractory compounds (Adediran et al., 2021).

Agro waste is continuously being explored as a reinforcement material for these AMCs. Although some studies have used these agro wastes with other synthetic materials (usually ceramics), forming a hybrid reinforcement for these metal matrix composites (Parveez et al., 2021; Kareem et al., 2021; Ikubanni et al., 2021). High silica agro-waste materials such as rice husk, mango seed shells, doum palm seed shells, etc. are abundantly found in Nigeria (Lewoyehu, 2021). These agro-wastes have been a source of environmental concern as their disposal poses risk to humans but they can also be harnessed and converted to silicon-based materials (Kavaz, 2022). The availability, low weight, and low cost are a drive for its use as reinforcement for these AMCs. It has been reported that for metal matrix composites, these agro wastes can either serve as direct precursors or can be ashed before further synthesis (Prempeh et al.,

2021). The produced ash serves as reinforcements in the development of the aluminum matrix composites. Some of the processes used in the development of these agro-waste ash reinforced AMCs are liquid filtration, double stir casting, rheo-casting, compocasting, etc. The simplicity, flexibility, and viability of the double stir cast method have made it the most used in this development process.

Accessing synthetic reinforcement materials in some societies like developing countries is a challenge. Therefore, agro-waste materials, which have proven to be a viable alternative must be developed. Different studies have been carried out on the use of agro-waste materials in the reinforcement of metal matrix composites. Adediran *et al.*, (2018) have successfully synthesized Si-based refractory compounds (SRC) from rice husk (RHs) via a carbothermal processing route. These SRCs comprise a good percentage of silicon carbide and other refractory compounds in their structures. Thus, making them a potential reinforcement material in the design of AMCs (Akbar *et al.*, 2020). Also, RHs possess a good percentage of silica, hematite, and alumina as major refractory oxides in their structure (Adediran *et al.*, 2021).

Taguchi's robust design of experiment method has successfully been applied to processes and systems in order to obtain the optimum performance with a spend of minimal resources (Samuel *et al.*, 2021). The Taguchi optimization method involves the study of the effect of varied parameters with the S/N ratio. These S/N ratios are either expressed in the form of the "higher the better", "the lower the better", or "the nominal the best." In the case of wear rate where the lower wear rate is expected to be achieved, "the lower the better" S/N ratio is applied. S/N ratio for the lower the better is expressed in Equation 1.

$$S/N_{LB} = -10 * \log_{10} \left(\frac{1}{n} \sum_{i=1}^n y_i^2 \right)$$

1

Where S/N_{LB} represents the signal to noise ratio for the lower the better characteristics, y represents the responses and n is the number of runs.

There appears to be sparse literature on the characterization of AMCs reinforced with Si-based refractory compounds derived from Mango seed shells upon its abundance in Nigeria. The current study attempts to explore the mechanical and microstructural characteristics of aluminum metal matrix composites developed from Si-based refractory compounds of the Mango seed shell. This present work takes advantage of the availability of the mango seed shell to develop a mango seed shell ash reinforced Al-Si-Mg-MSSA composite with varying compositions of the MSSA content of 0%, 5%, 10%, and 15%. The surface properties of the composite materials are studied. The data from these findings would add to the existing database of cost-effective and technically efficient secondary reinforcement phases to improve aluminum metal matrix composites.

2.0 Experimentation

Materials and Equipment

The metal used as a matrix used for the composite production is Al-Si-Mg. The aluminum metal was obtained from Aluminum wires which were procured from the northern cable company (NOCACO) Kaduna state. Magnesium and Silicon were obtained in their powdered form from a metal shop in Jos, Plateau State Nigeria. Some of the equipment used include charcoal furnace and stirrer, Digital weigh balance, cope and drag, a die cavity mold, scanning electron microscope (SEM), wear testing machine, and optical microscope. The mango seed (agro-waste) were obtained from consumed ripened mango fruits.

Methodology

MSSA Preparation

The Mango seeds shells collected were collected, washed thoroughly, dried in the sun for three days, decorticated manually to remove the seed from the shell, and ground into powder. The powder of MSSA was packed in a steel box and ashed in an air-tight condition in a furnace at 600°C for four hours to obtain the ash. The ash was sieved using a sieve size of 250µm. These ash are used in the processing of the Al-Si-Mg-MSSA composite.

Production of the Al-Si-Mg Alloy

The stir cast method was employed in the production of the Aluminum alloy used. Using a charcoal furnace, the aluminum wires were charged into the crucible. The wires were melted completely, and 7% silicon was added upon superheating to 700°C. In other to obtain uniform distribution of the silicon, the molten alloy was mixed thoroughly for 5 minutes and removed from the furnace and 0.3% magnesium was added. Samples were cast from the melt in form of bars for further development.

Al-Si-Mg-MSSA Production

The Al-7%Si-0.3%Mg bars already produced were reheated to 660°C in the crucible. The Mango seed shell ash was heated to 120°C to dry off possible moisture absorbed or oxides and other and other volatile materials. The heated ash particles were activated by further heating the ash to 500°C. The MSSA was added to the molted aluminum alloy in varying proportions of 0%, 5%, 10%, and 15% respectively as according to the Taguchi orthogonal design. The crucible in which the bars were melted again was removed from the furnace and there was continuous stirring for 60 seconds with a stirring speed of 100rpm upon the addition of MSSA for dispersion of the ash in the aluminum alloy. The composite was then poured into a mold and left to cool at room temperature.

Wear Test

Wear test samples were fabricated with a length of 35mm and a diameter of 10mm and were subjected to abrasive wear conditions. The test was carried out according to the ASTM D 6079-97/EN 590 standards using the Anton Paar Strasse 208054 Wear testing machine.

Microstructural Characterization

The Inverted type Metallurgical Microscope (Nikon, Range-X50 to X1500) at 200 times magnification was used for the microstructural study. Scanning Electron Microscopy (SEM) was used for the study of the surface morphology of fractured surfaces of the developed composites. The scanning electron microscope was operated at 15 kV and a working distance of 15 mm, selected areas of interest were focused and micrographs were taken as reported in Ramezani *et al.*, (2020) and Hoseinzadeh *et al.*, (2017). Before the microscopic examination, the samples were metallographically prepared using a series of grinding and polishing steps. Samples were then etched using Keller's reagent (1.0 ml HF, 1.5 ml HCl, 2.5 ml HNO₃, 95 ml water).

3.0 Results And Discussion

Optimization of Al-Si-Mg/MSSA Particulate Composite for Low Wear Rate

The wear rate of the developed composites are presented in Table 1

Table 1
Wear rate of the Al-Si-Mg composites

Runs	Parameter Settings				Wear Rate	
	Stir. Time (sec.)(A)	Pro. Temp. (°C)(B)	MSSA (wt. %)(C)	Part. Size (µm)(D)	Mean (mm ³ /N/m)	S/N (dB)
1	30	690	5	100	0.04499	26.9377
2	60	720	5	75	0.02248	32.9641
3	90	750	5	50	0.01538	36.2609
4	120	780	5	25	0.02036	33.8244
5	60	750	10	100	0.03131	30.0863
6	30	780	10	75	0.01348	37.4062
7	120	690	10	50	0.01783	34.9770
8	90	720	10	25	0.02371	32.5014
9	90	780	15	100	0.01788	34.9526
10	120	750	15	75	0.01628	35.7669
11	30	720	15	50	0.05062	25.9136
12	60	690	15	25	0.03671	28.7043
13	120	720	20	100	0.01318	37.6017
14	90	690	20	75	0.01614	35.8419
15	60	780	20	50	0.02452	32.2096
16	30	750	20	25	0.04225	33.0632
				Mean	0.02432	33.0632

Table 1 shows the wear rate of the developed Al-Si-Mg/MSSA particulate composite at different runs (combinations). It also depicts the Wear Rate properties of the materials through the experimental runs carried out during the study and the signal-to-noise ratio. From Table 1, the wear rate general mean and the S/N ratio mean of the developed Al-Si-Mg/MSSA composites are 0.02432mm³/N/m and 33.0632dB respectively. The S/N ratio was calculated from the lower the better performance characteristics for the Wear Rate.

Table 2
Wear Rate Response Table

Level	Stir. Time		Pro. Temp.		MSSA		Part. Size	
	Mean Wear Rate (mm ³ /N/m)	S/N Wear Rate (dB)	Mean Wear Rate (mm ³ /N/m)	S/N Wear Rate (dB)	Mean Wear Rate (mm ³ /N/m)	S/N Wear Rate (dB)	Mean Wear Rate (mm ³ /N/m)	S/N Wear Rate (dB)
1	0.0258	32.5	0.02684	32.39	0.03784	29.44	0.02892	31.62
2	0.02158	33.74	0.01709	35.49	0.02875	30.99	0.02750	32.25
3	0.03037	31.33	0.02709	32.34	0.01828	34.89	0.02631	32.4
4	0.02402	33.28	0.03076	30.63	0.01691	35.54	0.01906	34.6
Delta	0.00879	2.41	0.01366	4.87	0.02092	6.11	0.00986	2.98
Rank	4	4	2	2	1	1	3	3

Table 2 is the response Table for the wear rate of the developed composites where the wear rate of the composite was 0.02580mm³/N/m, 0.02158mm³/N/m, 0.03037mm³/N/m, and 0.02402mm³/N/m with S/N ratios of 32.50dB, 33.74dB, 31.33dB, and 33.28dB at stirring time of 30s, 60s, 90s, and 120s respectively. At processing temperatures of 630°C, 640°C, 650°C and 680°C, the mean wear rate was 0.02684mm³/N/m, 0.01709mm³/N/m, 0.02709mm³/N/m, and 0.03076mm³/N/m with S/N ratios of 32.39dB, 35.49dB, 32.34dB, and 30.63dB respectively. The mean wear rate under the influence of MSSA content 5%, 10%, 15% and 20% were 0.03784mm³/N/m, 0.02875mm³/N/m, 0.01828mm³/N/m, and 0.01691mm³/N/m with S/N ratios of 29.44dB, 30.99dB, 34.89dB, and 35.54dB respectively. The wear rate in respect to the particle size of MSSA at 100µm, 75µm, 50µm, and 25µm, were 0.02892mm³/N/m, 0.02750mm³/N/m, 0.02631mm³/N/m, and 0.01906mm³/N/m at means and 31.62dB, 32.25dB, 32.40dB and 34.60dB at S/N ratios. The stirring time had the highest rank with a difference between the highest and lowest mean wear rate as 0.00879 mm³/N/m and the MSSA reinforcement had a difference between the highest and lowest mean wear rate as 0.00986mm³/N/m.

Figure 1 shows the effect of stirring time on the wear rate of the Al-Si-Mg/MSSA composite. There was a wear rate reduction with an increase in stirring time from 30s to 60s. Figure 1 shows the lowest mean Wear Rate of 0.02158mm³/N/m at means and 33.74dB at S/N ratio on a stirring time of 60s and highest Wear Rate at 90s. Generally, it is observed that the wear rate increased with the increase in stirring time beyond 60s. But at a much higher stirring time, i.e. greater than 90s, the wear rate reduced. This is not disconnected from the fact that with more stirring time, there will be increased dispersion of the secondary phases in the alloy as reported in Ayar et al., (2021).

The effect of processing temperature on the wear rate of Al-Si-Mg/MSSA composite is shown in Figure 2. It shows that the wear rate of the composite decreases with the increased processing temperature from 690°C to 720°C where the lowest wear rate was observed. This is due to the ease of solidification within

these temperatures. Beyond 720°C, the wear rate increased with an increase in pouring temperature due to the formation of voids by bubbling at these higher temperatures.

Effect of MSSA Content on the Wear Rate of Al-Si-Mg/MSSA Composite

Figure 3 shows the variation of wear rate with MSSA content. It shows that the wear rate reduces with an increase in MSSA content. The ash particles form a lubricating point at surfaces and an increase in these particle content increases the wear inhibition mechanism. The rate of reduction of wear is linear until 15% MSSA content where the rate of reduction in wear rate is reduced and this is due to the increase in more crystalline materials within the phases as observed by Stalin et al., (2021).

Effect of Particle Size on the Wear Rate of Al-Si-Mg/MSSA Composite

Figure 4 shows the variation of wear rate with particle size from 25µm-100µm. It shows that the wear rate decreases with a decrease in particle size in agreement with Vishal *et al.*, (2021) who stated that particle size governs the mechanical and tribological characteristics of such composite materials. At 100µm particle size, the peak of wear rate was observed to be 0.02892mm³/N/m. The best (lowest) wear rate (0.01906mm³/N/m) was observed to be at the smallest particle size of 25µm.

Figures 5-8 show the interaction effect of MSSA content (in weight percent), stirring time, processing temperature, and particle size. It could be observed that the highest wear rate, was observed at MSSA content between 12-18% and at a low stirring time of less than 60s. So also, the wear rate was observed to be the highest at MSSA content between the range of 12-18% and pouring temperature of 700-740°C. The highest wear rate was also observed at particle size within 30-70µm. Figure 8 shows the interaction between stirring time and particle size.

Analysis of Variance for the Wear Rate of Al-Si-Mg/MSSA Composite

Table 3
Analysis of Variance of Means for Wear Rate of AL-SI-MG/MSSA Composite

Source	DF	Adj SS	Adj MS	F	P	Percentage Contribution
Stirring Time (sec.) (A)	1	0.00002	0.00002	0.25	0.627	1.07
Processing Temperature (°C) (B)	1	0.000014	0.000014	0.17	0.686	0.75
MSSA reinforcement (wt. %) (C)	1	0.000715	0.000715	8.94	0.012	38.09
Particle Size (µm)(D)	1	0.000248	0.000248	3.11	0.106	13.21
Error	11	0.00088	0.00008			
Total	15	0.001877				

Table 3 shows the analysis of variance of the wear rate of Al-Si-Mg/MSSA composite for the various factors that were considered. The MSSA reinforcement has the highest percentage contribution to the wear rate of the composite. Implying that for the factors considered, the MSSA content contributes 38.09% to the wear rate. In other to reduce the wear rate, the MSSA content must be taken into consideration. The particle size contributed 13.21% to the wear rate of the composite material. With a P-Value less than 0.05 at a 95% confidence level, the MSSA content was observed to be a significant factor in the wear rate of the developed material.

Optimal Wear Rate of Al-Si-Mg/MSSA Composite

The optimal development combination of the factors for the development of Al-Si-Mg/MSSA composite for low wear is obtained from the response table. From Figure 1-4, it could be observed that the best (optimum) development parameters are stirring time of the 60s, processing temperature at 720°C, MSSA content of 20%, and particle size of 25µm. Which is A2B2C4D4. The optimal Wear Rate of the composite was predicted using Equation 2 to be 0.00168mm³/N/m at means and 40.1804dB at S/N Ration.

$$W_{Opt} = W_{St} + W_{Pr} + W_{Ma} + W_{Ps} - 3W_m$$

2

Where W_{opt} is the optimal wear rate, W_{Pr} is the lowest wear rate at the processing temperature, W_{Ma} is the lowest wear rate at varied mango seed shell ash content, and W_{Ps} is the lowest wear rate at different varied particle sizes.

To confirm the predicted optimum Wear Rate, a confirmatory experiment was carried out with the optimum set of parameters A2B2C4D4. The confidence interval calculated from Equation 3 showed that the interval lies on ±0.00021mm³/N/m of the predicted optimal Wear Rate.

$$Confidenceinterval = \sqrt{f_{\alpha(1, DOF_e)} \times V_e \times \left(\frac{1}{E} + \frac{1}{R} \right)}$$

3

$f_{\alpha(1, DOF_e)}$ is the f ratio tabulated (between 1 and DoF_e i.e. the degree of freedom of error), V_e is the variance of error, and R is the number of replications. E=total number of experiments/(1+total degree of freedom of factors).

A composite material was developed with the optimum material combination A2B2C4D4 which is Al-Si-Mg/MSSA composite with stirring time, processing temperature, MSSA content, and particle size of 60s, 720°C, 20%, and 25µm respectively obtained as the best or optimal composition. The wear rate test was carried out on three samples. The result of the confirmation test is presented in the observation Table 4.

Table 4
Observation of Wear Rate Confirmation Test

S/N	Trial Number			Average Wear Rate (mm ³ /N/m)	S/N Ratio (dB)
	1	2	3		
1	0.00151	0.00151	0.00153	0.001517	56.38

Table 4 shows the result of the confirmatory test. The average Wear Rate (mean) of the confirmatory material was 0.001517mm³/N/m which was within the confidence interval such that $(0.00168\text{mm}^3/\text{N/m} - 0.00021 \text{ mm}^3/\text{N/m}) < 0.001517\text{mm}^3/\text{N/m} < (0.00168\text{mm}^3/\text{N/m} + 0.00021 \text{ mm}^3/\text{N/m})$ which is $0.00147\text{mm}^3/\text{N/m} < 0.001517\text{mm}^3/\text{N/m} < 0.00189\text{mm}^3/\text{N/m}$. The predicted optimum wear rate and the experimental optimum wear rate is presented in Table 5.

Table 5
Confirmatory Test Result for the Optimal Wear Rate of Al-Si-Mg/MSSA Composite

	Optimal Process Parameter Settings	Predictive Values	Experimental Values
S/N ratio (dB)	A2B2C4D4	40.1804	56.38
Mean Wear Rate mm ³ /N/m)	A2B2C4D4	0.00168	0.001517

Wear Modeling

A mathematical model for the combination of stirring time (A), Processing temperature (B), MSSA content (C), and Particle size (D) was derived from regression analysis carried out using the Minitab® 19 statistical software which was used for the prediction of the Wear Rate properties of the developed composite. The regression analysis model is presented in Table 6.

Table 6
Regression analysis model for Wear Rate

Term	Coef	SE Coef	T-Value	P-Value	VIF
Constant	0.04207	0.0091	4.62	0.001	
Stirring time (s)(A)	0.000173	0.000965	0.18	0.861	1
Processing Temp. (°C)(B)	0.000435	0.000386	1.13	0.284	1
MSSA Content (wt.%(C)	-0.000146	0.000039	-3.8	0.003	1
Particle Size (µm)(D)	-0.000615	0.000386	-1.59	0.139	1
R-Square=0.9032					

Regression Equation

Wear Rate = 0.538 - 0.00689 A + 0.000134 B - 0.00332 C - 0.00073 D (4)

Table 6 shows the regression analysis model for the wear rate. Also, equation 4.6 shows the regression model for the wear rate for the factors considered. R-Square value of 90.32% shows the accuracy of the regression model developed. It explains the suitability of the model in predicting the wear rate under the factors considered. A comparison of the predicted wear rate using the regression equation and the experimental values of the Al-Si-Mg/MSSA composite is compared in Figure 9.

Microstructural Analysis

Microstructural Analysis Using SEM

Figure 10 shows an almost uniform distribution of Al-Si-Mg alloy consisting of primary grains of α -Al solid solution (white) surrounded by interdendritic regions of coarse plates of Al-Si eutectic (deep black) in which various intermetallic phases are present including the precipitates of Mg_2Si intermetallic compound. etched with Keller's solution.

At 5%wt content, the mango shell ash (MSSA) particles reinforcement in the grain boundaries of the Al-Si-Mg matrix was observed. The structure reveals the precipitates of Mg_2Si and platelet of eutectic Si particles in α -Al matrix with (MSSA) particles.

Also, at 15% wt MSSA content, there was more presence of the reinforcement within the grain boundaries of the Al-Si-Mg matrix. The structure revealed the precipitates of Mg_2Si and networks of eutectic Si particles in α -Al matrix with a fairly uniform distribution of mango seed shell ash (MSSA) particles. This showed that there was good interfacial bonding between the 15% MSSA particles and the Al-Si-Mg matrix. The presence of magnesium in the matrix helps in enhancing the wettability of the MSSA particles in the metal matrix.

A higher percentage of the presence of reinforcement within the grain boundaries of Al-Si-Mg matrix was observed at the 20% wt content of MSSA reinforcement. The structure revealed the precipitates of Mg_2Si and networks of eutectic Si particles in α -Al matrix with non-uniform distribution of mango seed shell ash particles (MSSAp). The excess presence of reinforcement (MSSAp) beyond 15% resulted in a poor distribution of MSSAp in the Aluminium matrix. This made the composite slurry, too thick, and reduce the fluidity of the molten metal which adversely affected the mechanical and physical properties of this sample. etched with Keller's solution.

Conclusion

1. Al-Mg-Si /MSSAp composite was successfully developed using the stir casting technique and the samples were used for the wear test.
2. The addition of Mango Seed Shell Ash particulate to Al-Si-Mg has resulted in microstructural changes which confirm that it can be used as a reinforcement for AMCs.
3. The optimal wear rate of the MSSA reinforced Al-Si-Mg composite is $0.001517\text{mm}^3/\text{N/m}$ at stirring time, processing temperature, MSSA content, and particle size of 60s, 720°C , 20%, and $25\mu\text{m}$.

4. The wear behavior of the developed composite has been successfully modeled with a prediction accuracy of 90.32%.

Declarations

Funding: This research did not receive any funding

Conflicts of interest/Competing interests: On behalf of all authors, the corresponding author states that there is no conflict of interest.

Availability of data and material: Not applicable

Code availability: Not applicable

Ethics approval: Not applicable

Consent to participate: Not applicable

Consent for publication: Not applicable

References

1. Adediran AA, Alaneme KK, Oladele IO, &Akinlabi ET (2021) Microstructural characteristics and mechanical behaviour of aluminium matrix composites reinforced with Si-based refractory compounds derived from rice husk. *Cogent Eng* 8(1):1897928
2. Akbar HI, Surojo E, Ariawan D, Prabowo AR, Imanullah F (2021) Fabrication of AA6061-sea sand composite and analysis of its properties. *Heliyon*, 7(8), e07770
3. Ayar MS, George PM, Patel RR (2021), February Advanced research progresses in aluminium metal matrix composites: An overview. In *AIP Conference Proceedings* (Vol. 2317, No. 1, p. 020026). AIP Publishing LLC
4. Guo B, Song M, Zhang X, Liu Y, Cen X, Chen B, Li W (2021) Exploiting the synergic strengthening effects of stacking faults in carbon nanotubes reinforced aluminum matrix composites for enhanced mechanical properties. *Compos Part B: Eng* 211:108646
5. Hosseinzadeh F, Rastegar SO, Ashengroph M, Gu T (2021) Ultrasound-assisted Fenton-like reagent to leach precious metals from spent automotive catalysts: process optimization and kinetic modeling. *International Journal of Environmental Science and Technology*,1–10
6. Ikubanni PP, Oki M, Adeleke AA, Omoniyi PO (2021) Synthesis, physico-mechanical and microstructural characterization of Al6063/SiC/PKSA hybrid reinforced composites. *Sci Rep* 11(1):1–13
7. Kareem A, Qudeiri JA, Abdudeen A, Ahammed T, Ziout A (2021) A review on AA 6061 metal matrix composites produced by stir casting. *Materials* 14(1):175
8. Kavaz D (2022) Synthesis of silica nanoparticles from agricultural waste. *Agri-Waste and Microbes for Production of Sustainable Nanomaterials*. Elsevier, pp 121–138

9. Lewoyehu M (2021) Comprehensive review on synthesis and application of activated carbon from agricultural residues for the remediation of venomous pollutants in wastewater. *J Anal Appl Pyrol* 159:105279
10. Parveez B, Maleque MA, Jamal NA (2021) Influence of agro-based reinforcements on the properties of aluminum matrix composites: a systematic review. *J Mater Sci* 56(29):16195–16222
11. Prempeh CO, Formann S, Schliermann T, Dizaji HB, Nelles M (2021) Extraction and Characterization of Biogenic Silica Obtained from Selected Agro-Waste in Africa. *Appl Sci* 11(21):10363
12. Raj P (2021) Optimization of parameters in SiC production via Acheson Process—a hot model study (Doctoral dissertation)
13. Ramezani Dana H, El Mansori M, Barrat M, Seck CA (2021) Tensile behavior of additively manufactured carbon fiber reinforced polyamide-6 composites. *Polymer-Plastics Technology and Materials*, 1–18
14. Salur E, Aslan A, Kuntoğlu M, Acarer M (2021) Effect of ball milling time on the structural characteristics and mechanical properties of nano-sized Y₂O₃ particle reinforced aluminum matrix composites produced by powder metallurgy route. *Adv Powder Technol* 32(10):3826–3844
15. Samuel BO, Sumaila M, Dan-Asabe B (2021) Manufacturing of a natural fiber/glass fiber hybrid reinforced polymer composite (PxGyEz) for high flexural strength: an optimization approach. *The International Journal of Advanced Manufacturing Technology*, 1–12
16. Stalin B, Ravichandran M, Sudha GT, Karthick A, Prakash KS, Asirdason AB, Saravanan S (2021) Effect of titanium diboride ceramic particles on mechanical and wear behaviour of Cu-10 wt% W alloy composites processed by P/M route. *Vacuum* 184:109895
17. Vishal K, Rajkumar K, Annamalai VE (2021) Wear and tribofilm characterization of bamboo CNT (B-CNT)-peek composite with incremental blending of submicron synthetic diamond particles. *Wear* 466:203556
18. Wang M, Li Y, Chen B, Shi D, Umeda J, Kondoh K, Shen J (2021) The rate-dependent mechanical behavior of CNT-reinforced aluminum matrix composites under tensile loading. *Mater Sci Engineering: A* 808:140893
19. Xie Y, Meng X, Mao D, Qin Z, Wan L, Huang Y (2021) Homogeneously dispersed graphene nanoplatelets as long-term corrosion inhibitors for aluminum matrix composites. *ACS Appl Mater Interfaces* 13(27):32161–32174
20. Zhu C, Su Y, Wang X, Sun H, Ouyang Q, Zhang D (2021) Process optimization, microstructure characterization and thermal properties of mesophase pitch-based carbon fiber reinforced aluminum matrix composites fabricated by vacuum hot pressing. *Compos Part B: Eng* 215:108746

Figures

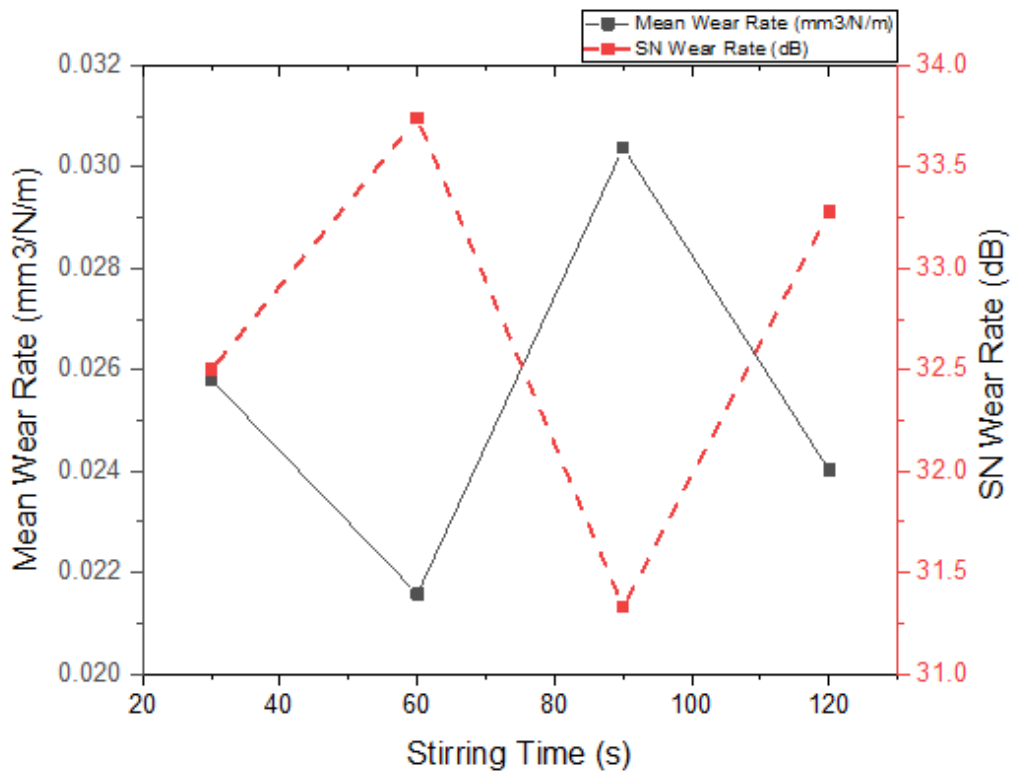


Figure 1

Variation of Wear Rate Mean and S/N ratio with Stirring Time

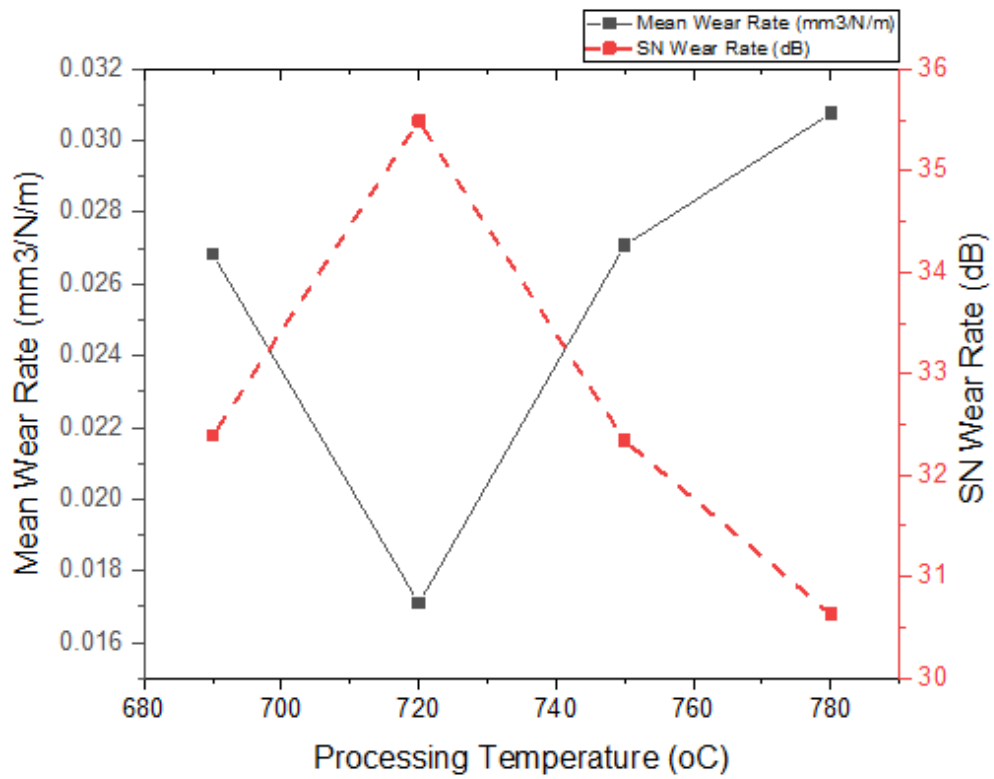


Figure 2

Variation of Wear Rate Mean and S/N ratio with Processing Temperature

Figure 3

Variation of Wear Rate Mean and S/N ratio with MSSA Content

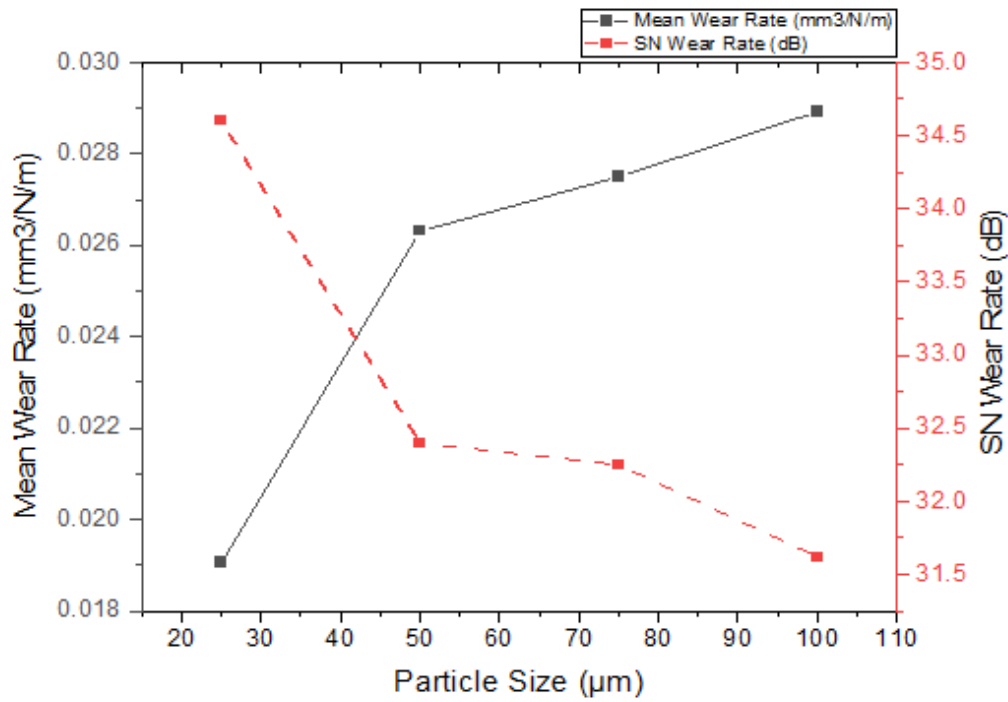


Figure 4

Variation of Wear Rate Mean and S/N ratio with Particle Size

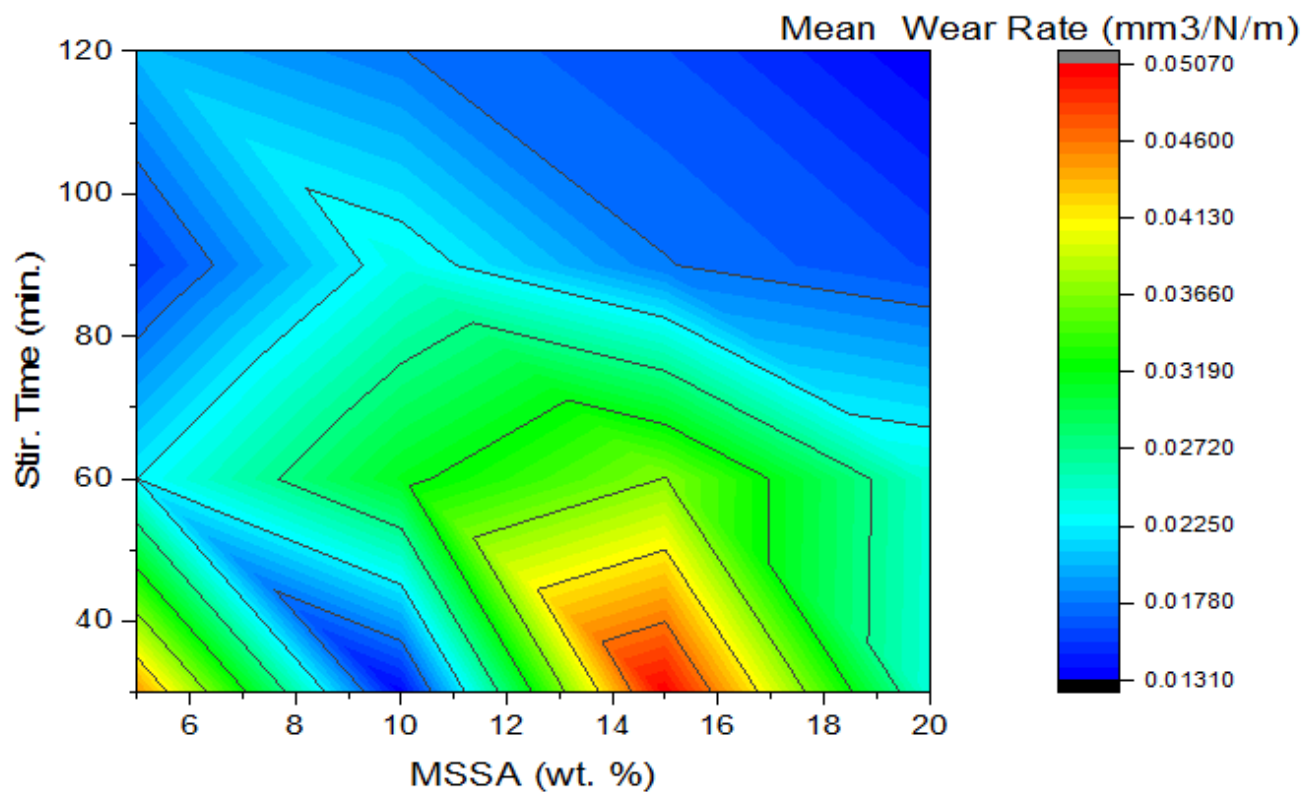


Figure 5

Interaction of MSSA content with stirring time

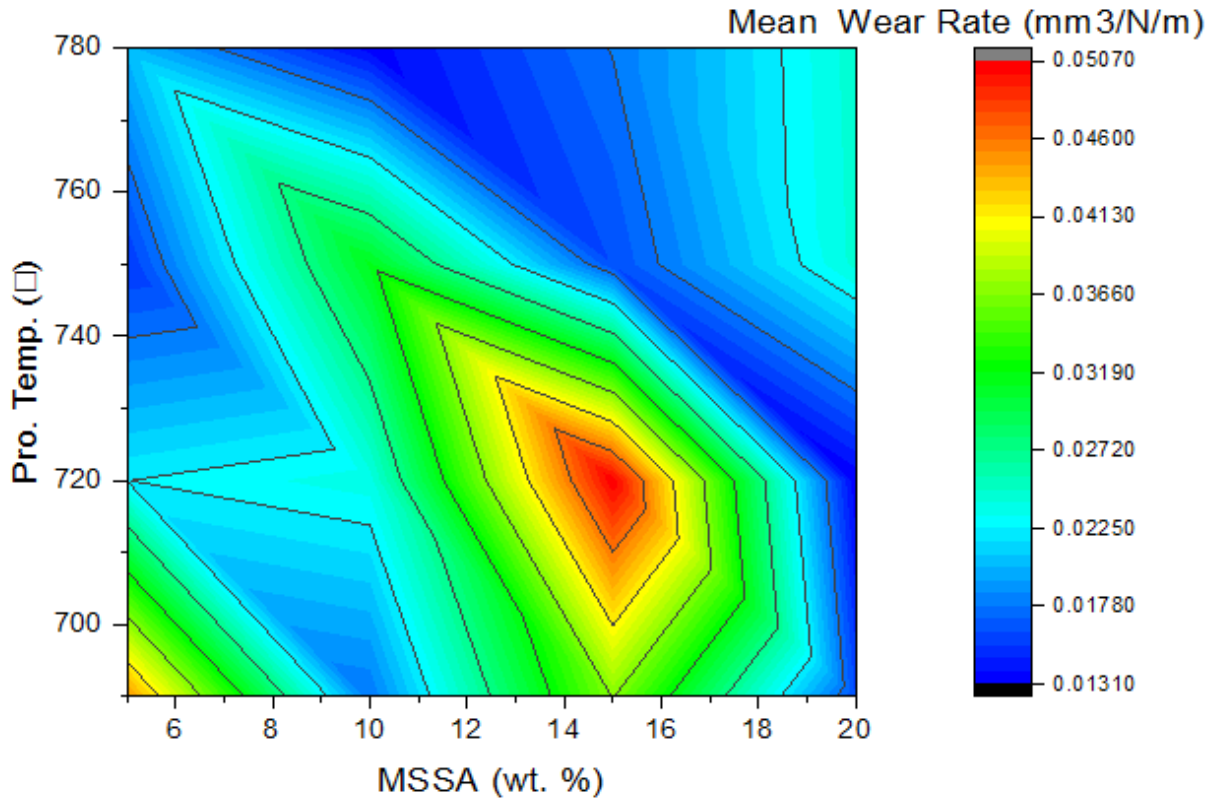


Figure 6

Interaction of MSSA content with processing temperature

Figure 7

Interaction of MSSA content with particle size

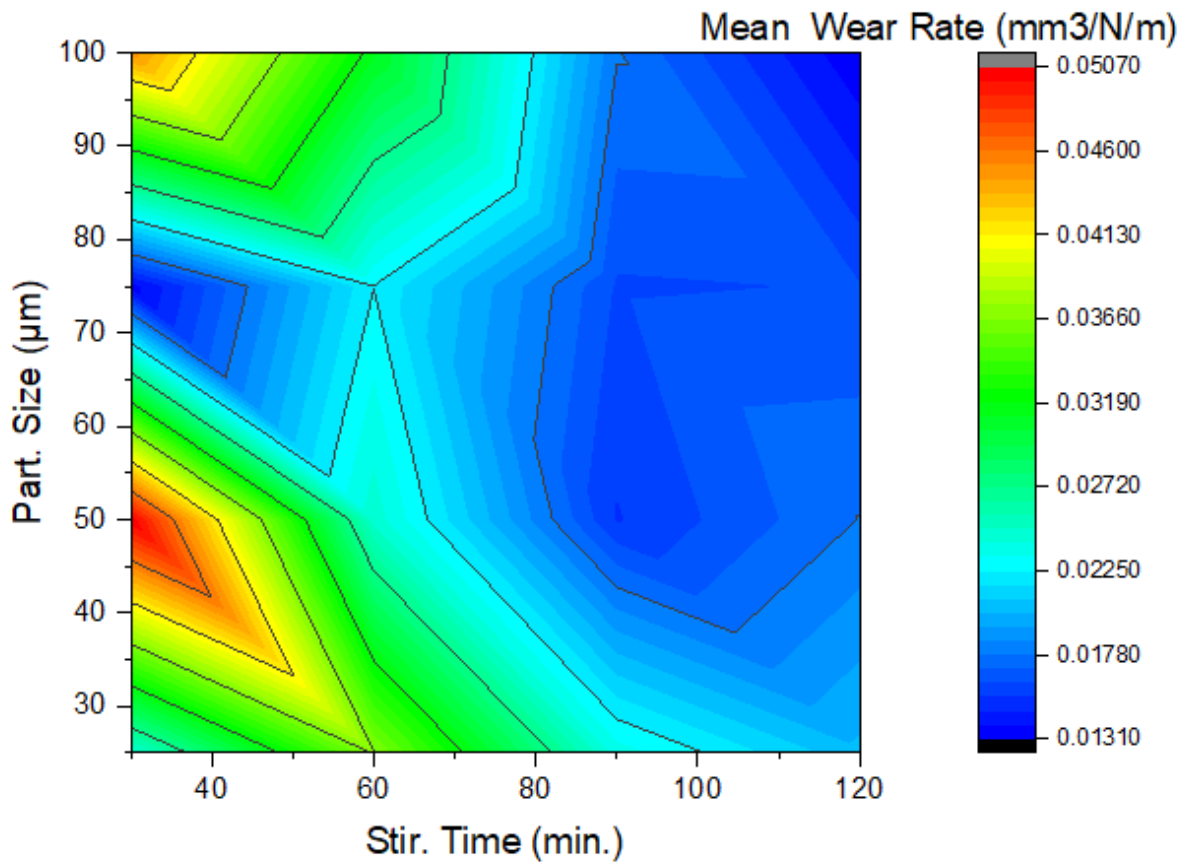


Figure 8

Interaction of stirring time with particle size

Figure 9

Predicted and experimental Wear Rate of Al-Si-Mg/MSSA composites

Figure 10

SEM Micrographs of the Al-Si-Mg composites